Available online at BCREC website: https://bcrec.id

Bulletin of Chemical Reaction Engineering & Catalysis, 14 (3) 2019, 568-578

Research Article

CO_2 Reforming of Methane over $LaNiO_3$ Perovskite Supported Catalysts: Influence of Silica Support

D. Sellam[1]*, K. Ikkour[1], S. Dekkar[1], H. Messaoudi[2], T. Belaid[3], A.C. Roger[4]

[1]*Laboratoire de Chimie Applique et de Genie Chimie, Université Mouloud Mammeri (UMMTO), Tizi-ouzou, Algeria*
[2]*Laboratoire des Matériaux Catalytiques et Catalyse en Chimie Organique, Faculté de Chimie, Université Science and Technology Houari Boumediene (USTHB), Algeria*
[3]*Université A. Mira Bejaia, Algeria*
[4]*Institut de Chimie et Procédés pour l'Énergie, l'Environnement et la Santé, CNRS-Université de Strasbourg, France*

Received: 24th October 2018; Revised: 21st May 2019; Accepted: 24th May 2019; Available online: 30th September 2019; Published regularly: December 2019

Abstract

The study presents the dry reforming of methane using natural Kaolin silica as catalyst support. The silica-supported $LaNiO_3$ perovskite catalysts ($20LaNiO_3/SiO_2$ and $40LaNiO_3/SiO_2$) and bulk $LaNiO_3$ catalyst were synthesized by auto-combustion method. The resulting catalysts were characterized by X-ray diffraction (XRD), N_2 adsorption - desorption isotherm measurement, scanning electron microscopy (SEM) and temperature-programmed reduction (TPR). After reduction at 700 °C, they were used as catalysts for the reaction of dry reforming of methane into synthesis gas at atmospheric pressure at 800 °C. The reduced $40LaNiO_3/SiO_2$ exhibited high catalytic activity. This result was attributed to the small Ni metallic particles obtained from the reduced perovskite highly dispersed on the support and the good reducibility. The increase of reduction temperature at 800 °C resulted in a further enhancement of the catalytic performance of $40LaNiO_3/SiO_2$ catalyst. Copyright © 2019 BCREC Group. All rights reserved

Keywords: Methane; Syn gas; $LaNiO_3$ supported catalyst; kaolin silica.

How to Cite: Sellam, D., Ikkour, K., Dekkar, S., Messaoudi, H., Belaid, T., Roger, A.C. (2019). CO_2 Reforming of Methane over $LaNiO_3$ Perovskite Supported Catalysts: Influence of Silica Support. *Bulletin of Chemical Reaction Engineering & Catalysis*, 14(3): 568-578 (doi:10.9767/bcrec.14.3.3472.568-578)

Permalink/DOI: https://doi.org/10.9767/bcrec.14.3.3472.568-578

1. Introduction

Carbon dioxide reforming of methane (DRM) has received considerable attention because both CH_4 and CO_2, greenhouse gases contribute to global warming. This process could be industrially advantageous, yielding a syngas with a H_2/CO ratio close to 1, suitable for Fischer-Tropsch synthesis to liquid hydrocarbons and for production of valuable oxygenated chemicals [1]. Dry reforming ($CH_4 + CO_2 \rightarrow 2H_2 + 2CO$ $\Delta H^{\circ}_{r\,298} = 247\ kJ/mol$) is a highly endothermic reaction necessitating high reaction temperatures at which coke formation and sintering of catalysts become serious problems [2].

Noble metal based catalysts (Ru, Rh, Pd, Ir, and Pt) have been reported to be the most active and show better coke resistance in this reaction [3,4], but their high costs limited their use as catalysts. Previous studies showed that Ni metal could possibly replace the expensive noble

* Corresponding Author.
E-mail: sdjamila2015@gmail.com (D. Sellam);
Telp.: +213777030433

metal catalysts [5,6]. Because of the availability of Ni metal and for economic reasons, it is more desirable, from the industrial point of view, to develop Ni-based catalysts. However, the main problem is the rapid deactivation of the Ni-based catalysts due to a strong carbon deposition and sintering of metal particles [7].

It is reported that the insertion of nickel into a well-defined structure, like the perovskites [8], hexaaluminates [9], spinels [10] or in a solid solutions [11], can reduce its deactivation. In dry reforming reaction, the active site is metallic transition metal [12]. The mixed-oxide of perovskite type (ABO_3) as catalyst precursor allows after reduction the formation of small metal particles highly dispersed at the surface of a basic support. This small particle size reduces carbon formation and improves the activity and stability of the catalyst [13]. A well-known example is the reduction of a $LaNiO_3$ perovskite precursor to form Ni/La_2O_3. Previous reports suggested that these materials are active for dry reforming [14,15]. However, the heat treatment of these oxides generally leads to the formation of catalysts with low specific surface area (generally below 10 $m^2.g^{-1}$) [16,17], which limits the potential application of these oxides. Many different procedures, including co-precipitation [17], sol-gel [18], Pechini [19], auto-combustion [20], are proposed in the literature to produce perovskite with smaller crystal size and higher surface area. However, most of the synthesis method allow producing crystal size between 15 nm and 25 nm. Consequently, surface area remains limited. One way to solve this problem and to generate nanocrystals is to disperse the perovskite-type oxide on a support which possesses a high specific surface area and thermal stability, and prevents the sintering of the metal [21,22]. Ordered, silica mesostructures are intrinsically preferred catalyst supports due to their high specific surface area and large pore size. In addition, the confined space inside the pore channels will aid the well-controlled formation of nanoparticles of catalytically active materials. Rivas *et al.* [21] synthesized a series of Ni-based perovskite-type oxides $LaNiO_3$, $La_{0.8}Ca_{0.2}NiO_3$, and $La_{0.8}Ca_{0.2}Ni_{0.6}Co_{0.4}O_3$, as a catalyst precursors in highly ordered mesoporous SBA-15 silica support. The incorporation of the oxides into the mesoporous silica resulted in enhanced metal–support interaction that then increased the Ni reduction temperature.

Improved conversions and selectivities were observed at low temperature and no significant loss in CH_4 conversion was reported at 700 °C for 24 h in the case of mesoporous catalysts. Wang *et al.* [23] synthesized $LaNiO_3$ perovskite catalysts supported on various silica-based mesoporous supports ($LaNiO_3$/SBA-15, $LaNiO_3$/MCM-41 and $LaNiO_3/SiO_2$) with different pore structures. Their catalytic performances were measured in methane dry reforming. $LaNiO_3$/MCM-41 exhibited the highest initial catalytic activity, owing to higher Ni dispersion, while $LaNiO_3$/SBA-15 was superior to $LaNiO_3$/MCM-41 in the long-term stability (60 h), which could be due to the stable silica matrix limiting the agglomeration of nickel species.

In comparison, the carbon deposition was responsible for the significant decrease in catalytic activity of the $LaNiO_3/SiO_2$ sample. Dacquin *et al.* [24] used an in situ auto-combustion synthesis route to produce nanoparticle nickel oxide (~3 nm). They prepared highly dispersed metallic Ni nanoparticles from $LaNiO_3$/SBA nanoprecursor reduction. The catalytic performance for syngas production was doubled compared to bulk $LaNiO_3$. These materials were found to be stable at 700 °C for 48 h. Moradi *et al.* [25] studied the effects of Ni loading and preparation methods on the performance of perovskite-type oxides ($LaNiO_3$) dispersed on γ-Al_2O_3 for the CO_2 reforming of CH_4 into synthesis gas. The catalyst with 20 wt% Ni prepared by the impregnation method using ethanol as solvent and citric acid exhibited the best activity and stability at 800 °C for 75 h time-on-stream. Recently, natural clays stand as interesting catalytic supports in dry reforming of methane reaction, since they are naturally available and low-cost materials. Akri *et al.* [26] used natural illite clay as catalyst support for nickel for the autothermal reforming of methane. The presence of lanthanum markedly improved the catalytic stability for 24 h of reaction at 800°C. Liu *et al.* [27] used Tunisian natural clay as support to prepare nickel based catalysts modified with Fe and Cu for dry reforming of methane. They found that the Cu-modified catalyst exhibited a good activity at 850°C.

In the present work, we report the use of natural silica obtained from siliceous by-product of Algerian kaolin as support of perovskite-type oxides with different $LaNiO_3$ loadings. The aim of the study was to investigate the catalytic performances of these materials with respect to the dry reforming of methane into synthesis gas.

The by-product of kaolin is rich in silica easily available of low cost and exhibits a good

Copyright © 2019, BCREC, ISSN 1978-2993

thermal stability, needed for methane dry reforming reaction. The use of this natural silica as catalytic support has never been reported before.

2. Materials and Method

2.1 Materials

Siliceous by-product of Algerian kaolin used as the raw material to produce the silica support. The chemicals used were as follows: lanthanum nitrate hexahydrate (99.9% $La(NO_3)_3.6H_2O$), nickel nitrate hexahydrate (99 % $Ni(NO_3)_2.6H_2O$), glycine (99% $C_2H_5NO_2$), sulfuric acid (96% H_2SO_4), Hydrochloric acid (37% HCl) and distilled water. All reagents were purchased from Sigma-Aldrich.

2.2 Catalysts Preparation

2.2.1 Silica support

The starting material was siliceous by-product of kaolin. Its composition is detailed in Table 1. It is rich in silica (about 92%). The preparation of silica from siliceous by- product of kaolin has been already reported [28]. In order to remove the iron oxides, a batch (250 g) of by-product was stirred in 500 mL of H_2SO_4 (4 M) over night at room temperature. Stirring was maintained until a heterogeneous mixture (liquid and paste) was obtained. This mixture was washed with an abundant quantity of distilled water and then dried at 100 °C for 24 hours. The obtained product was ground to obtain a fine powder to which a mass of 52.29 g of sodium carbonate has been added. The solid mixture was then calcined at 1000 °C. After calcination, a quantity (10 g) of the obtained compound was dissolved in 500 mL of hot distilled water (50 °C) in order to prepare hydrated sodium silicates. To remove sodium, hydrochloric acid solution (2 M) was then added. The obtained silica gel SiO_2 was washed several times with distilled water until the absence of ions Cl^- in the washing water and then dried at 100 °C for 24 hours.

2.2.2 Perovskite supported catalysts

A series of lanthanum-nickel supported mixed oxides $xLaNiO_3/SiO_2$ (where x is the weight loading of $LaNiO_3$ in the catalyst and is fixed at 20 and 40 wt %) were synthesized by the in-situ auto-combustion procedure [29]. In a first step, nitrate precursors with a mass ratio of lanthanum nitrate to nickel nitrate of 3:2 were dissolved in a limited volume of distilled water (20 mL). After complete dissolution at room temperature, glycine was then added to the nitrate solution at a NO_3^-/glycine molar ratio of 1, the solutions were mixed and agitated constantly for about 2h. The freshly calcined support (1.0 g) was thereafter slowly impregnated with this solution. After 2 h of agitation, the temperature of the mixture increased up to 100 °C until complete evaporation of water, and a powder was obtained. Then, glycine auto-ignition occurred on increasing the temperature to 280 °C. The powder obtained was finally calcined at 700 °C (ramp 1 $°C.min^{-1}$) for 4h for residual carbonaceous elimination. The catalysts nomenclature is given as shown: $20LaNiO_3/SiO_2$ and 40 $LaNiO_3/SiO_2$ samples contained respectively 20 wt. % and 40 wt. % of $LaNiO_3$. The bulk perovskite $LaNiO_3$ was prepared as reference using the same procedure (auto-combustion).

2.2 Catalyst Characterization

The synthesized solids were characterized by X-ray powder diffraction (XRD) at 2θ between 10° and 80° with a 0.020° step and an acquisition time of 0.80 s at each step for crystalline phase detection, using a Bruker AXS-D8 Advanced equipment (Cu-Kα = 0.15406 nm). The crystalline phases were identified by comparing with the database. The crystallite size was calculated from the full width at half maximum of the most intense diffraction peaks using Scherrer's equation. Textural properties were obtained by N_2-sorption experiment at −196 °C on a Micromeritics ASAP 2420 apparatus. Specific surface areas were calculated according to BET procedure. Prior to analysis, samples were out gassed at a temperature of 250 °C. The BJH method was applied for determination of pore volume and pore size distribution. The supported catalysts and the support morphologies were observed by scanning electron microscopy (SEM) using a Philips XL-30 ESEM microscope.

Table 1. Chemical composition and calcination losses of siliceous by-product of kaolin [28]

Oxides	SiO_2	Al_2O_3	Fe_2O_3	CaO	Na_2O	MgO	K_2O	TiO_2	P_2O_5	LOI	Total
Weight (%)	92.72	3.42	0.71	0.20	0.05	0.14	0.69	0.09	0.09	1.30	99.41

Copyright © 2019, BCREC, ISSN 1978-2993

Temperature programmed reduction (TPR) was carried out for temperatures ranging from 50 to 800 °C with a Micromeritics Autochem II 2920 instrument using 50 mg of catalyst. Catalysts were reduced under 10% H_2 balanced with Ar at flow rate of 50 mL.min^{-1} from 50 to 800 °C with heating rate of 5 °C.min^{-1}. Before analysis, the catalysts were pretreated for one hour at their calcination temperature (700 °C) under oxygen (30 mL.min^{-1}) in order to activate the catalyst by removing water and impurities deposited on the surface. The consumption of hydrogen was followed by TCD.

2.3 Catalytic activity

The catalysts performances were evaluated at atmospheric pressure in a U quartz reactor (internal diameter of = 6.0 mm). All samples were tested for methane dry reforming reaction, after an in-situ reduction under pure hydrogen (10 mL.min^{-1}) at 700 °C for 1 h. The mass of catalyst was adjusted to 10 mg of $LaNiO_3$ for catalytic comparison. The SiO_2 support alone was inactive at 800 °C. After stabilization of the reacting flow (CH_4/CO_2 = 1/1, at a GHSV of 600 L.h^{-1}.g^{-1}), the activity was measured each 30 min for 4 hours at reaction temperature of 800 °C. The reactants (CH_4 and CO_2) and products (CO and H_2) were analyzed on line using TCD gas chromatograph equipped with a Carbosieve column. The catalytic performance was evaluated by CH_4 and CO_2 conversions, CO and H_2 yields and H_2/CO molar ratio and was calculated using Equations (1-5).

$$Conversion(XCH_4\,\%) = \frac{n_{(CH_4)in} - n_{(CH_4)out}}{n_{(CH_4)in}} \times 100 \quad (1)$$

$$Conversion(XCO_2\,\%) = \frac{n_{(CO_2)in} - n_{(CO_2)out}}{n_{(CO_2)in}} \times 100 \quad (2)$$

$$Yield\ (YH_2\,\%) = \frac{n_{(H_2)out}}{2\,n_{(CH_4)in}} \times 100 \quad (3)$$

$$Yield(YCO_2\,\%) = \frac{n_{(CO_2)out}}{n_{(CH_4)in} - n_{(CO_2)in}} \times 100 \quad (4)$$

$$Molar\ ratio(H_2/CO) = \frac{n_{(H_2)produced}}{n_{(CO)produced}} \quad (5)$$

3. Results and discussion

3.1 Physicochemical characterization

Table 2 shows the specific surface areas of the catalysts after synthesis. The specific sur-

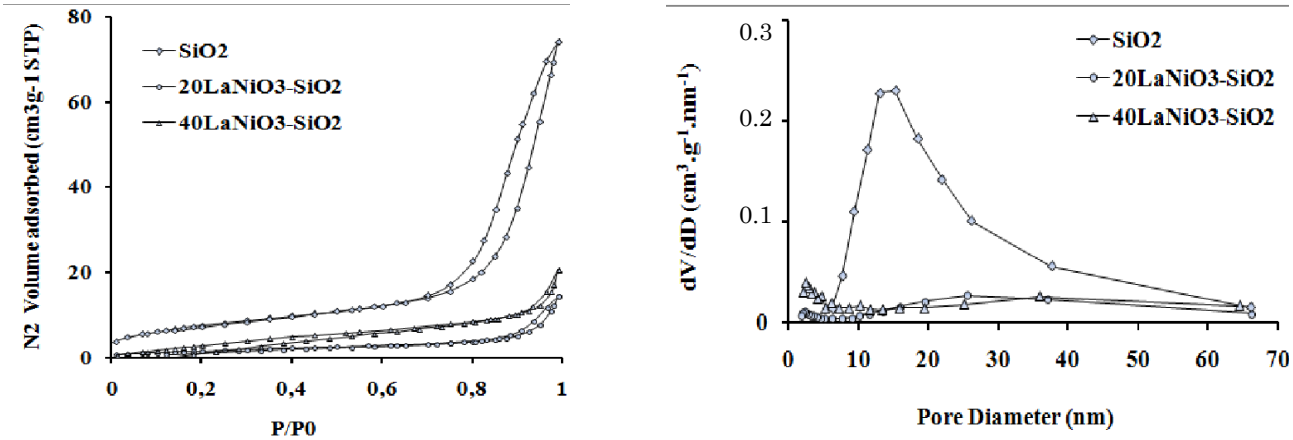

Figure 1. N_2 adsorption–desorption isotherms and pore size distribution obtained for SiO_2 support, 20 $LaNiO_3/SiO_2$ and 40$LaNiO_3/SiO_2$ catalysts.

Table 2. BET surface area, pore volume, pore diameter and NiO crystallite size of the catalysts

Sample	Surface area (m^2/g)	Pore volume (cm^3/g)	Pore Diameter (nm)	NiO Crystal size (nm)
$LaNiO_3$	9	-	-	18
SiO_2	56	0.108	16	-
20$LaNiO_3/SiO_2$	7	0.016	10	54
40$LaNiO_3/SiO_2$	32	0.023	7	15

Copyright © 2019, BCREC, ISSN 1978-2993

face area of the SiO_2 support is 56 $m^2.g^{-1}$. This value is relatively low for a support. High calcination temperature might be the reason for this low surface area [16]. The specific surface area of the support decreased after impregnation with the mixed oxide. This decrease is not proportional to the loading of the mixed oxide. Low specific surface area is calculated for $20LaNiO_3/SiO_2$ (7 $m^2.g^{-1}$) catalyst. The low surface area could be related to the high particles size (54 nm) [30]. However, a relatively high surface area is observed for $40LaNiO_3/SiO_2$ (32 $m^2.g^{-1}$) compared to the bulk perovskite $LaNiO_3$ (9 $m^2.g^{-1}$). On the other hand, a decrease in the pore volume and pore size is significant, probably due to the partial blockage of the pores originally present by the mixed oxides [24]. The isotherms are different for the support and the supported perovskite catalysts (Figure 1). The SiO_2 support presents a well defined hysteresis loop characteristic of type IV isotherms according to BDDT (Brunauer, Deming, Deming and Teller) classification, which indicates that the support is mesoporous. The similar isotherm was observed for Ce-promoted illite clay based catalyst [31]. However, for the supported catalysts $20LaNiO_3/SiO_2$ and $40LaNiO_3/SiO_2$ the isotherms seem to be likely of type-II. These results agree with those reported by Akri *et al.* [31]. The corresponding pore size distribution (Figure 1) confirms the mesoporisity of the support, as highlighted by pore size distribution at 16 nm.

The XRD patterns of the catalysts are displayed in Figure 2. The XRD patterns of the bulk catalyst $LaNiO_3$ shows the main diffraction lines at 2θ = 31.9°, 45.7°, and 58.7°, characteristic of the rhombohedral structure of $LaNiO_3$ (JCPDS file n° 01-088-0633), which confirms the presence of a perovskite-type structure. The perovskite structure is also observed for the supported catalyst $20LaNiO_3/SiO_2$ with low peak's intensity. These characteristic peaks are not observed in the XRD patterns of $40LaNiO_3/SiO_2$, therefore, the perovskite structure was not formed. However, for this catalyst, two phases of single oxide are formed which correspond to La_2O_3 and NiO. The XRD pattern shows the main diffraction peaks at 22.4°, 26.7°, 29.7°, and 52.6° characteristic of La_2O_3 cubic structure (JCPDS file n° 03-065-3185) and main diffraction peaks at 37.2°, 43.1°, and 62.8° characteristic of the NiO cubic structure (JCPDS n° 01-089-7130). These two phases (NiO and La_2O_3) are also observed for the $20LaNiO_3/SiO_2$ catalyst in addition to the perovskite. The XRD pattern of the silica support shows main reflections at 20.9°, 26.7°, 36.6°, 42.5°, 50.2°, and 60.1° characteristic of SiO_2 hexagonal structure. The presence of quartz is also detected (JCPDS n°01-085-0504) in the supported catalysts. We notice that some characteristic peaks of cubic NiO and La_2O_3 overlap with those of hexagonal SiO_2.

The $20LaNiO_3/SiO_2$ catalyst has a low specific surface area with a large NiO particle size. This result can be explained by the formation of the mixed oxide $LaNiO_3$ which is generally well crystallized, which has a low specific surface area and the presence of the free oxide NiO. This free oxide promotes the formation of

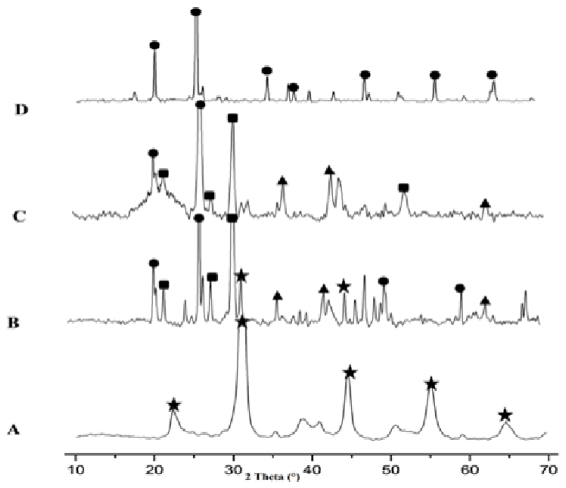

Figure 2. X-ray patterns of studied catalysts: $LaNiO_3$ bulk (A), $20LaNiO_3/SiO_2$ (B), $40LaNiO_3/SiO_2$ (C) and SiO_2 support (D). (●) SiO_2, (★) $LaNiO_3$, (▲) NiO, (■) La_2O_3

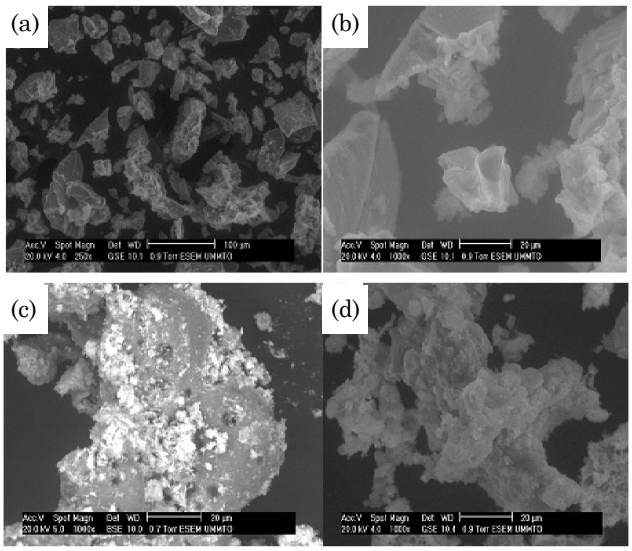

Figure 3. SEM micrograph obtained for SiO_2 (a,b), $40LaNiO_3/SiO_2$ (c) and $20LaNiO_3/SiO_2$ (d).

Copyright © 2019, BCREC, ISSN 1978-2993

large particles, especially when the interactions with the support are weak. On the other hand, for the catalyst $40LaNiO_3/SiO_2$, the formation of the mixed oxide was not recorded and the formation of NiO is well dispersed at the surface of the support.

SEM micrographs of calcined samples are illustrated in Figure 3. The silica powder appears under small particles form with irregular shape. These particles are bonded to each other to form small aggregates (Figure 3a and 3b). After impregnation with the mixed oxide $LaNiO_3$, the morphology changed as shown in Figure 3c and 3d. The supported catalyst $40LaNiO_3/SiO_2$ appears in the form of nanoscale particles irregularly dispersed on the surface of SiO_2 silica which present some porosity (micropores). While for the 20 $LaNiO_3/SiO_2$ catalyst, it is noted that on the zone observed, the micrographs reveal the formation of agglomerates with irregular form.

3.2 Temperature-Programmed Reduction (TPR)

Reducibility of the different solids was studied in order to ensure a sufficient reduction pretreatment before catalytic test. Numerous authors reported that the active species in dry reforming of methane are the metallic Ni^0 particles present on the surface of the catalyst [12,32]. The reduction of the bulk $LaNiO_3$ sample shows two main steps (Figure 4b), corresponding to the reduction of the trivalent nickel Ni^{3+} into divalent nickel Ni^{2+} at low temperature (~300°C) with formation of $La_2Ni_2O_5$ brownmillerite phase followed by the reduction of Ni^{2+} in $La_2Ni_2O_5$ to its metallic state Ni^0 at high temperature (~ 435 °C). The intensity of the second peak equals twice that of the first peak indicating the formation of $LaNiO_3$. The reduction of Ni^{3+} in $LaNiO_3$ to Ni^0 is summarized by two following reactions:

$$2LaNiO_3 + H_2 \rightarrow La_2Ni_2O_5 + H_2O$$
$$La_2Ni_2O_5 + 2H_2 \rightarrow La_2O_3 + 2Ni + 2H_2O$$

The supported catalysts exhibit different TPR profiles with respect to the bulk perovskite $LaNiO_3$. The TPR profiles of $20LaNiO_3/SiO_2$ (Figure 4a) presents three main reduction zones that characterize three steps of reduction. The first one occurs at around 340°C, which is related to the reduction of NiO to Ni^0. These species are present on the perovskite surface. Rudolfo *et al.* also reported a peak of reduction at 573 K, which is attributed to NiO on the surface [33]. The second step is observed at ~ 500 °C, due to the reduction of Ni^{3+} in the perovskite to Ni^{2+} which generates the formation of the $La_2Ni_2O_5$ phase, this last being reduced at ~ 630 °C as indicates the third peak. These reduction steps are carried out according to the following reactions:

$$NiO + H_2 \rightarrow Ni^0 + H_2$$
$$2LaNiO_3 + H_2 \rightarrow La_2Ni_2O_5 + H_2O$$
$$La_2Ni_2O_5 + 2H_2 \rightarrow La_2O_3 + 2Ni + 2H_2O$$

Comparing the reduction profiles to those of $LaNiO_3$ bulk, we can see that the peaks related to the reduction of perovskite are small with low intensity and shifted to higher temperature, indicating that the reduction of perovskite becomes difficult because of the strong interaction between perovskite and silica support [24]. The TPR profile of $40LaNiO_3/SiO_2$ is totally different. It shows one large reduction zone at ~ 400 °C corresponding to the reduction of Ni^{2+} to Ni^0 of NiO species on the catalyst surface. As it is observed, this peak of reduction is close to the second peak of reduction of $LaNiO_3$

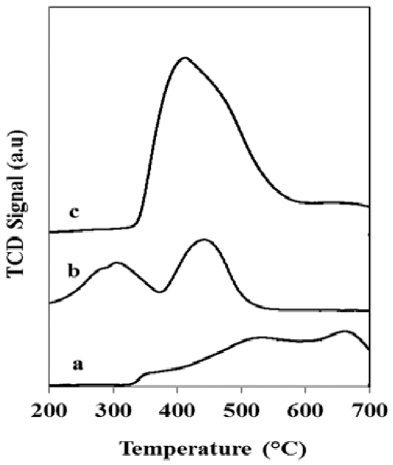

Figure 4. TPR profiles of $20LaNiO_3/SiO_2$ (a), $LaNiO_3$ bulk (b) and $40LaNiO_3/SiO_2$ (c) catalysts.

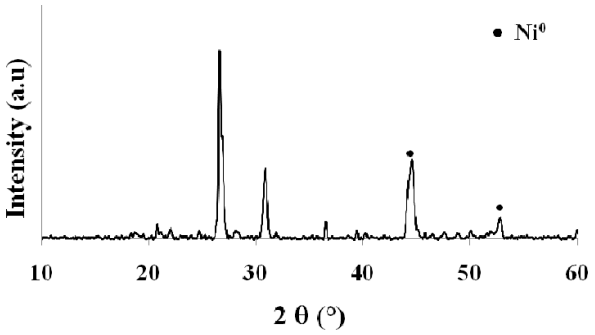

Figure 5. XRD patterns of reduced $40LaNiO_3$-SiO_2 catalyst at 800 °C.

Copyright © 2019, BCREC, ISSN 1978-2993

bulk perovskite. La_2O_3 is not reducible. For this supported catalyst, reduction profiles move to higher temperature. It is believed that reducibility of NiO species, in supported nickel catalysts, is highly affected by the nature of metal–support interaction [34,35]. Generally, when the interactions between NiO and support (SMSI) are strong, the main peak of reduction shifts to higher temperature, the reduction becomes very difficult, thus decreasing Ni reducibility. It also suggests the existence of better Ni dispersion comparing to non supported catalyst, but when the interactions (SMSI) are weak, the peak shifts to lower temperature; the reduction of metal becomes easier, thus increasing the Ni reducibility [24,27].

This study is in good correlation with the XRD studies confirming the presence of different phases. XRD patterns recorded on $40LaNiO_3/SiO_2$ reduced catalyst at 800 °C are reported in Figure 5. The presence of reduced Ni^0 is evidenced by reflections at $2\theta = 44.45°$ and 52°. Ni^0 crystal sizes were calculated applying Scherrer equation to the diffraction peak appearing at 44.45° of pure Ni(111) reflecting plane. The calculated value was around of 11 nm.

3.3 Catalytic Activity

After reduction at 700 °C for 1h under hydrogen, the prepared catalysts were tested in dry reforming of methane at 800 °C in a CO_2/CH_4 ratio equal to 1, under atmospheric pressure. The effect of the support and the $LaNiO_3$ loading on the catalytic properties of the perovskite were investigated. The CH_4 and CO_2 conversions as well as the CO and H_2 yields of reduced supported perovskite and bulk $LaNiO_3$ catalysts are shown in Figure 6. The $20LaNiO_3/SiO_2$ supported catalyst does not show any catalytic activity under reaction condition. The reason may be the low surface area and large particles size 54 nm (Table 1) or the

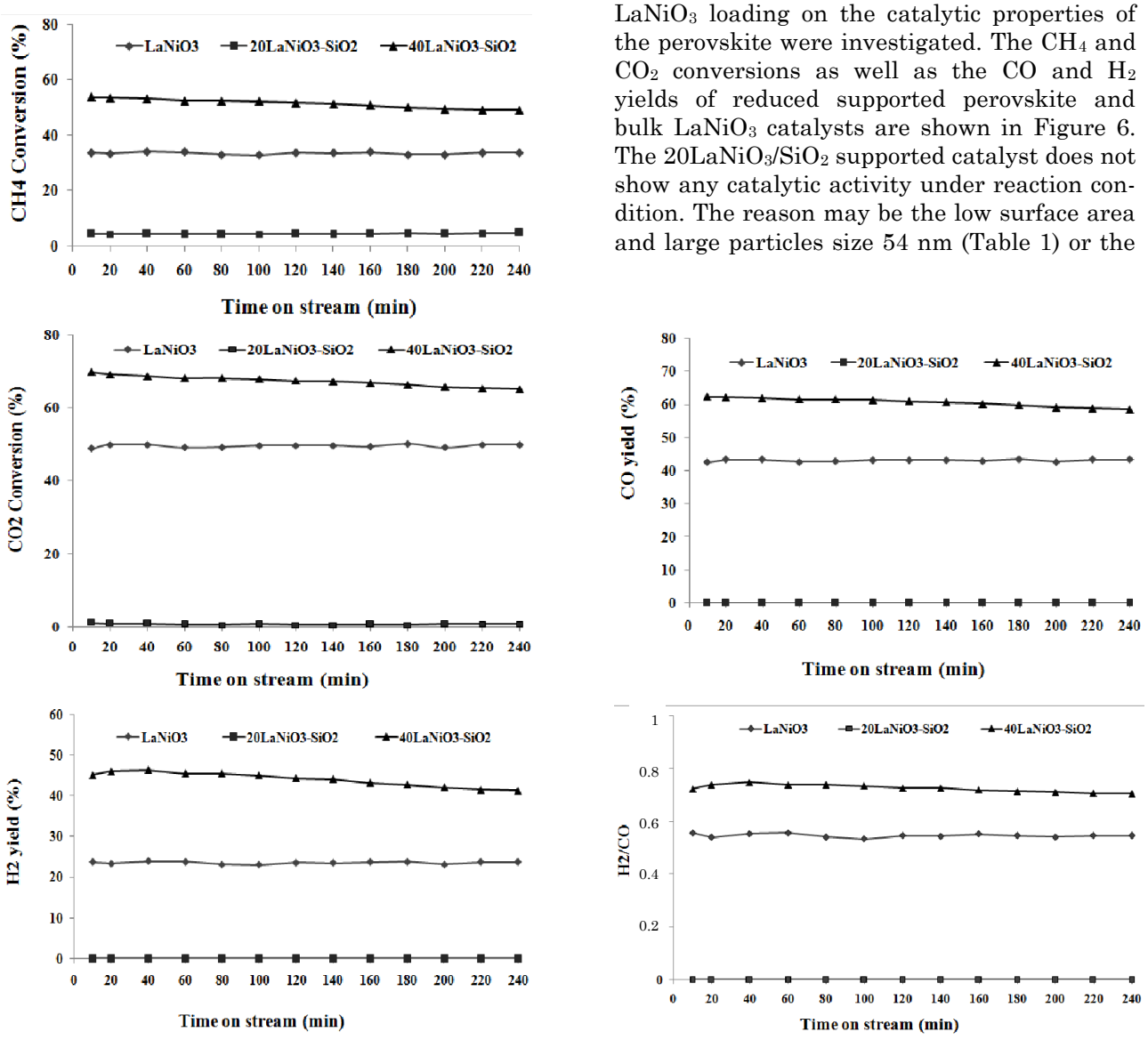

Figure 6. Catalytic performance of $LaNiO_3$, $20LaNiO_3/SiO_2$, and $40LaNiO_3/SiO_2$ reducted catalysts at 700°C in DRM reaction at 800 °C.

Copyright © 2019, BCREC, ISSN 1978-2993

low reducibility of the catalyst as shown by TPR profiles. These results are not in agreement with those obtained with $20LaNiO_3$/SBA supported catalyst [24]. The authors reported that the catalytic performance in dry reforming of methane of this catalyst was much better than that obtained with the bulk $LaNiO_3$. The catalyst had high surface area and Ni^0 nanoparticles size of about 3 nm. Liu *et al.* [36] showed that the addition of Al and Mn to Fe modified natural clay supported Ni catalysts increased the specific surface area and promoted Ni dispersion. Al-promoted catalysts improved the Ni reducibility and presented the best catalytic performance in dry reforming of methane compared to La and Mn-promoted catalysts. However, the $40LaNiO_3/SiO_2$ catalyst showed higher catalytic activity than the bulk perovskite $LaNiO_3$.

In this case, the methane and CO_2 conversions remained constant at around 50% (CH_4) and 65% (CO_2) after 3 h of time on stream. During the reaction, the conversion of CO_2 is higher than the conversion of methane, even the yield of CO is higher than that of H_2, the values of H_2/CO ratio near to 0.8 less than 1 and the formation of water, suggesting that besides methane dry reforming reaction, reverse water-gas shift reaction (RWGS: $CO_2 + H_2 \rightarrow CO + H_2O$) is also occurring. In general, CO_2 reforming of methane is typically accompanied by the simultaneous occurrence of a RWGS reaction [22,31]. The yield of CO is higher than that of H_2 (Figure 6), this confirms the presence of parallel reactions during dry reforming of methane. Some of them lead to carbon formation which leads to the deactivation of the catalyst. However, the presence of basic support such as La_2O_3 can improve the resistance to coke deposition [37]. We attribute the superior performance of 40 $LaNiO_3/SiO_2$ catalyst to the presence of nanocrystallites of nickel (15 nm Table 1), highly dispersed on the surface of silica support. Rivas *et al.* [21] reported that the $LaNiO_3$/SBA-15 catalyst had crystal size of about 9 nm and good activity for DRM. Moradi *et al.* [25] attributed the better activity of $LaNiO_3/Al_2O_3$ for DRM to high dispersion of metallic nickel crystals (14-50 nm) on the Al_2O_3 support. The good reducibility shown by high H_2 consumption and large peak of the 40 $LaNiO_3/SiO_2$ catalyst could be also the reason for its high catalytic efficiency in dry reforming of methane. Amin *et al.* [38] have found that Er- promoted Ni/Al_2O_3 catalyst showed more reducibility, which is the reason for its high catalytic efficiency in dry reforming of methane.

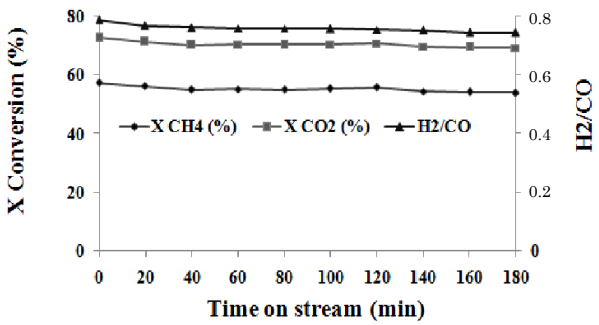

Figure 7. Catalytic performance of $40LaNiO_3/SiO_2$ after reduction at 800 °C in DRM reaction at 800 °C.

In order to confirm the effect of reducibility on the performance of $40LaNiO_3/SiO_2$ catalyst, reduction temperature at 800 °C was investigated. Figure 7 shows the results obtained in dry reforming of methane reaction experiments. From these results, we note that the increase of reduction temperature at 800 °C improves the catalytic activity of the catalyst. Methane and carbon dioxide conversions are higher than the ones obtained at reduction temperature of 700 °C. The conversions were maintained at around 55% and 70%, respectively for CH_4 and CO_2 after 3h of reaction. The H_2/CO ratio is slightly lower than unity. The CO_2 conversion, following the same trend, remains higher than the CH_4 conversion. This is mainly due to the occurrence of the reverse water gas shift reaction. This activity may be explained by the small nickel size generated after reduction at 800 °C which are highly dispersed at the surface of the support. Liu *et al.* [36] have found that the reduction temperature had a big influence on Ni crystal size. The natural clay based Ni-containing catalysts reduced at 900 °C had a smaller Ni crystal sizes than those reduced at 800 °C. No deactivation of the catalyst was observed during time on stream. According to Gallego *et al.* [20,39,40], the presence of La_2O_3 can improve the catalytic activity with increasing the basic sites, the surface Ni content and it can participate in dry reforming of methane by reacting with CO_2 to form $La_2O_2CO_3$ phase, able to gasify the carbon deposits formed to produce CO.

Copyright © 2019, BCREC, ISSN 1978-2993

4. Conclusions

In the present work, we investigated the effect of the natural support on the activity of a $LaNiO_3$ perovskite catalyst. The $LaNiO_3/SiO_2$ supported catalysts and $LaNiO_3$ were prepared by in-situ auto-combustion procedure. Their activity was tested in the dry reforming of methane (DRM) at 800 °C. The results showed that the use of kaolin silica as support plays a role of promoter in the physico-chemical and catalytic properties of the perovskite catalyst. It improved the physico-chemical and catalytic properties of the mixed oxide catalyst. Compared to the $LaNiO_3$ bulk, the $40LaNiO_3/SiO_2$ supported catalyst presented a relatively high surface area (32 $m^2.g^{-1}$) and small particle sizes (15 nm). Also, this latter exhibited the highest catalytic activity, which is probably attributed to the small Ni particle size high dispersed on the support and the good reducibility. The increase of reduction temperature at 800 °C results in an enhancement of the Ni dispersion on the silica surface and the high catalytic activity was obtained with 40 $LaNiO_3/SiO_2$ catalyst.

Acknowledgments

The authors gratefully acknowledge assistance from professor Anne Cécile Roger, Director of (Equipe Energie et Carburants pour un Environnement Durable ICPEES-ECPM, UMR CNRS, Strasbourg, France) laboratory for her help in the realization of this work. We thank the members of the laboratory whose conducted characterization analysis and catalytic tests.

References

[1] Stagg-Williams, S.M., Noronha, F.B., Fendley, G., Resasco, D.E. (2000). CO_2 reforming of CH_4 over Pt/ZrO_2 catalysts promoted with La and Ce oxides. *J. Catal.*, 194: 240–249.

[2] Valderrama, G., Kiennemann, A., Goldwasser, M.R. (2008). Dry reforming of CH_4 over solid solutions of $LaNi_{1-x}Co_xO_3$. *Catal. Today*, 133: 142-148.

[3] Tsang, S.C., Claridge, J.B., Green, M.L.H. (1995). Recent advances in the conversion of methane to synthesis gas. *Catal. Today*, 23: 3–15.

[4] Hou, Z., Chen, P., Fang, H., Zheng, X., Yashima, T. (2006). Production of synthesis gas via methane reforming with CO_2 on noble metals and small amount of noble-(Rh-) promoted Ni catalysts. *Int. J. Hydrogen Energy*, 31: 555-561.

[5] Basile, F., Fornasari, G., Trifiro, F., Vaccari, A. (2002). Rh–Ni synergy in the catalytic partial oxidation of methane: surface phenomena and catalyst stability. *Catal. Today*, 77: 215-223.

[6] Verykios, X.E. (2003). Catalytic dry reforming of natural gas for the production of chemicals and hydrogen. *Int. J. Hydrogen Energy*, 28: 1045-1063.

[7] Ashok, J., Kawi, S. (2013). Steam reforming of toluene as a biomass tar model compound over CeO_2 promoted Ni/CaO–Al_2O_3 catalytic systems. *Int. J. Hydrogen Energy*, 38: 13938–13949.

[8] Sagar, T.V., Padmakar, D., Lingaiah, N., Rao, K.S.R., Reddy, I.A.K., Prasad, P.S.Sai. (2017). Syngas production by CO_2 reforming of methane on $LaNi_xAl_{1-x}O_3$ perovskite catalysts: influence of method of preparation. *J. Chem. Sci.*, 129: 1787–1794.

[9] Ikkour, K., Sellam, D., Kiennemann, A., Tezkratt, S., Cherifi, O. (2009). Activity of Ni Substituted Ca-La-hexaaluminate Catalyst in Dry Reforming of Methane. *Catal. Lett.*, 132: 213–217.

[10] Gil-Calvo, M., Jiménez-González, C., de Rivas, B., Ortiz, J.I.G., Lopez-Fonseca, R. (2017). Hydrogen Production by Reforming of Methane over $NiAl_2O_4/Ce_xZr_{1-x}O_2$ Catalysts. *Chem. Eng. Trans.*, 57: 901-906.

[11] Manh Ha, Q.L., Armbruster, U., Atia, H., Schneider, M., Lund, H., Agostini, G., Radnik, J., Vuong, H.T., Martin, A. (2017). Development of Active and Stable Low Nickel Content Catalysts for Dry Reforming of Methane. *Catalysts*, 7: 157-174.

[12] Choudhary, V.R., Rane, V.H., Rajput, A.M. (1993). Selective oxidation of methane to CO and H_2 over unreduced NiO-rare earth oxide catalysts. *Catal. Lett.*, 22: 289-297.

[13] Nair, M.M., Kaliaguine, S., Kleitz, F. (2014). Nanocast $LaNiO_3$ Perovskites as Precursors for the Preparation of Coke-Resistant Dry Reforming Catalysts. *ACS Catal.*, 4: 3837−3846.

[14] Batiot-Dupeyrat, C., Valderrama, G., Meneses, A., Martinez, F., Barrault, J., Tatibouet, J.M. (2003). Pulse study of CO_2 reforming of methane over $LaNiO_3$. *Applied Catal. A: General*, 248: 143–151.

[15] Dama, S., Ghodke, S.R.., Bobade, R., Gurav, H.R., Chilukuri, S. (2018). Active and durable alkaline earth metal substituted perovskite catalysts for dry reforming of methane. *Applied Catal. B: Env.*, 224: 146-158.

[16] Khalesi, A., Arandiyan, H.R., Parvari, M. (2008). Effects of Lanthanum Substitution by Strontium and Calcium in La-Ni-Al Perov-

Copyright © 2019, BCREC, ISSN 1978-2993

skite Oxides in Dry Reforming of Methane. *Chin. J. Catal.*, 29: 960-968.

[17] Rivas, M.E., Fierro, J.L.G., Goldwasser, M.R., Pietri, E., Pérez-Zurita, M.J., Griboval- Constant, A., Leclercq, G. (2008). Structural features and performance of $LaNi_{1-x}Rh_xO_3$ system for the dry reforming of methane. *Applied Catal. A: Gen.*, 344: 10-19.

[18] Moradi, G.R., Rahmanzadeh, M., Khosravian, F. (2014). The effects of partial substitution of Ni by Zn in $LaNiO_3$ perovskite catalyst for methane dry reforming. *Journal of CO_2 Utilization*, 6: 7-11

[19] Su, Y.J., Pan, K.L., Chang, M.B. (2014). Modifying perovskite-type oxide catalyst $LaNiO_3$ with Ce for carbon dioxide reforming of methane. *Int. J. Hydrogen Energy*, 39: 4917-4925.

[20] Gallego, G.S., Marín, J.G., Batiot Dupeyrat, C., Barrault, J., Mondragón, F. (2009). Influence of Pr and Ce in dry methane reforming catalysts produced from $La_{1-x}A_xNiO_{3-\delta}$ perovskites. *Applied. Catal. A: Gen*., 369: 97-103.

[21] Rivas, I., Alvarez, J., Pietri, E., Perez-Zurita, M.J., Goldwasser, M.R. (2010). Perovskite-type oxides in methane dry reforming: Effect of their incorporation into a mesoporous SBA-15 silica-host. *Catal. Today*, 149: 388–393.

[22] Rabelo-Neto, R.C., Sales, H.B.E., Inocêncio, C.V.M., Varga, E., Oszko, A., Erdohelyi, A., Noronha, F.B., Mattos, L.V. (2018). CO_2 reforming of methane over supported $LaNiO_3$perovskite-type oxides. *Applied Catal. B: Env.*, 221: 349–361.

[23] Wang, N., Yu, X., Wang, Y., Chu, W., Liu, M. (2013). A comparison study on methane dry reforming with carbon dioxide over $LaNiO_3$ perovskite catalysts supported on mesoporous SBA-15, MCM-41 and silica carrier. *Catal. Today*, 212: 98–107.

[24] Dacquin, J.P., Sellam, D., Batiot-Dupeyrat, C., Tougerti, A., Duprez, D., Royer, S. (2014). Efficient and Robust Reforming Catalyst in Severe Reaction Conditions by Nanoprecursor Reduction in Confined Space. *ChemSusChem*, 7: 631-637.

[25] Moradi, G., Hemmati, H., Rahmanzadeh, M. (2013). Preparation of a $LaNiO_3/\gamma$-Al_2O_3 Catalyst and its Performance in Dry Reforming of Methane. *Chem. Eng. Technol.*, 36: 575–580.

[26] Akri, M., Pronier, S., Chafik, T., Achak, O., Granger, P., Simon, P., Trentesaux, M., Batiot- Dupeyrat, C. (2017). Development of nickel supported La and Ce-natural illite clay for autothermal dry reforming of methane: Toward a better resistance to deactivation. *Applied Catal. B: Env.*, 205, 519–531.

[27] Liu, H., Yao, L., Bel Hadj Taief, H., Benzina, M., Da Costa, P., Gálvez, M.E. (2018). Natural clay-based Ni-catalysts for dry reforming of methane at moderate temperatures. *Catal. Today*, 306: 51-57.

[28] Brahmi, D., Merabet, D., Belkacemi, H., Mostefaoui, T.A., Ait Ouakli, N. (2014). Preparation of amorphous silica gel from Algerian siliceous by-product of kaolin and its physico chemical properties. *Ceramics International*, 40: 10499-10503.

[29] Sellam, D., Bonne, M., Arrii-Clacens, S., Lafaye, G., Bion, N., Tezkratt, S., Royer, S., Marécot, P., Duprez, D. (2010). Simple approach to prepare mesoporous silica supported mixed-oxide nanoparticles by *in situ* autocombustion procedure. *Catal. Today*, 157: 131-136.

[30] Yang, E., Noha, Y., Ramesh, S., Lim, S., Moon, D. (2015). The effect of promoters in $La_{0.9}M_{0.1}Ni_{0.5}Fe_{0.5}O_3$ (M = Sr, Ca) perovskite catalysts on dry reforming of methane. *Fuel Process. Technol.*, 134: 404-413.

[31] Akri, M., Chafik, T., Granger, P., Ayrault, P., Batiot-Dupeyrat, C. (2016). Novel nickel promoted illite clay based catalyst for autothermal dry reforming of methane. *Fuel*, 178: 139–147.

[32] Liu, B.S., Au, C.T. (2003). Carbon deposition and catalyst stability over La_2NiO_4/γ-Al_2O_3 during CO_2 reforming of methane to syngas. *Appl. Catal. A. Gen.*, 244: 181-195.

[33] Rodulfo-Baechler, S.M.A., Pernia, W., Aray, I., Figueroa, H., Gonzalez-Cortes, S.L. (2006). Influence of lanthanum carbonate phases of $Ni/La_{0.98}Sr_{0.02}O_x$ catalyst over the oxidative transformation of methane. *Catal. Lett.*, 112: 231–237.

[34] Naeem, M.A., Al-Fatesh, A.S., Abasaeed, A.E., Fakeeha, A.H. (2014). Activities of Ni-based nano catalysts for CO_2–CH_4 reforming prepared by polyol process. *Fuel Process. Technol*. 122: 141–152.

[35] Tao, K., Shi, L., Ma, Q., Wang, D., Zeng, C., Kong, C., Wu, M., Chen, L., Zhou, S., Hu, Y., Tsubaki, N. (2013). Methane reforming with carbon dioxide over mesoporous nickel–alumina composite catalyst. *Chem. Eng. J.*, 221: 25–31.

[36] Liu, H., Bel Hadjltaief, H., Benzina, M., Gàlvez, M.E., Da Costa, P. (2019). Natural clay based nickel catalysts for dry reforming of methane: On the effect of support promotion (La, Al, Mn). *Int. J. Hydrogen Energy*, 44(1): 246-255.

[37] Barros, B.S., Kulesza, J., de Araújo Melo, D.M., Kienneman, A. (2015). Nickel-based catalyst precursor prepared via microwave-

Copyright © 2019, BCREC, ISSN 1978-2993

induced combustion method: Thermodynamics of synthesis and performance in dry reforming of CH_4. *Mat. Res.*,18: 732-739.

[38] Amin, M.H., Putla, S., Bee Abd Hamid, S., Bhargava, S.K. (2015). Understanding the role of lanthanide promoters on the structure–activity of nanosized Ni/-Al_2O_3 catalysts in carbon dioxide reforming of methane. *Applied Catal. A: Gen.*, 492: 160–168.

[39] Istadi, I., Anggoro, D.D., Amin, N.A.S., Ling, D.H.W. (2011). Catalyst deactivation simulation through carbon deposition in carbon dioxide reforming over Ni/CaO-Al_2O_3 catalyst. *Bull. Chem. React. Eng. Catal*. 6(2): 129-136

[40] Gallego, G.S., Batiot-Dupeyrat, C., Barrault, J., Mondragon, F. (2008). Dual Active-Site Mechanism for Dry Methane Reforming over Ni/La_2O_3 Produced from $LaNiO_3$ Perovskite. *Ind. Eng. Chem. Res*, 47: 9272–9278.

Copyright © 2019, BCREC, ISSN 1978-2993